

The impact of AEM system configuration on inversion results

E.Tretyakova¹, D.Khliustov², F.Lazarev³

1. Institute of Control Sciences
Russia, ekaterina_tretikova@mail.ru

2. Institute of Control Sciences
Russia, hlustov.d@gmail.com

3. Norilsk branch of A.P. Karpinsky Institute
Russia, nf@karpinskyinstitute.ru

BIOGRAPHY

E. Tretyakova is a geophysicist in Geotechnologies Inc. and junior researcher in V. A. Trapeznikov Institute of Control Sciences.

D. Khliustov is a geophysicist in Geotechnologies Inc. and junior researcher in V. A. Trapeznikov Institute of Control Sciences.

F. Lazarev is the CEO of the Norilsk branch of A.P. Karpinsky Institute

SUMMARY

There exist several configurations of airborne electromagnetics (AEM) systems. For example, one may have transmitter and receiver fixed or towed, coaxial or separated, attached to helicopter or airplane. Moreover, the system may collect data in time domain, frequency domain or both. Each system has its benefits and drawbacks: towed ones are less influenced by primary field due to large distance between transmitter and receiver than those with fixed geometry, and time domain data is usually believed to be better suited for deep objects exploration, while frequency domain data are mostly concerned with near-surface region.

This paper is devoted to comparison of three system configuration. Namely, EM4H has four frequencies and can be either towed by a helicopter or a fixed wing aircraft, and EQUATOR collects data both in time- and in frequency domain and can only be towed by a helicopter. All three configurations have been tested on one profile, and the comparison of inversion results is given.

Key words: AEM data inversion, frequency domain, time domain

INTRODUCTION

The Earth's upper part crust exploration in large areas is carried out using AEM surveys. It is a geophysical method used for mineral exploration in diverse conditions (Telford, 1990). The difference between

possible approaches to this task lies both in the design of the transmitter and the receiver, and in the method of compensating for various interferences.

There exist several configurations of airborne electromagnetics systems (Legault, 2015, Moilanen, 2022, Whitford, 2023). Some of them have fixed transmitter and receiver coils, which leads to relative positioning being known and lower qualification demanded from pilot. However, in this configuration the receiver coil is strongly influenced by the primary field, thus demanding wider dynamic range of measurements. Other systems are towed, with either both transmitter and receiver attached to cable or transmitter fixed on an aircraft. We are talking in particular about the EQUATOR system and various modifications of the EM4H system.

The EM4H (Volkovitskiy et al., 2008) installed on an airplane or a helicopter is a cost-effective conductivity mapping system well suited for regional mineral exploration, groundwater resource evaluation, geological mapping, detailed survey of potential economic deposits (Figure. 1).

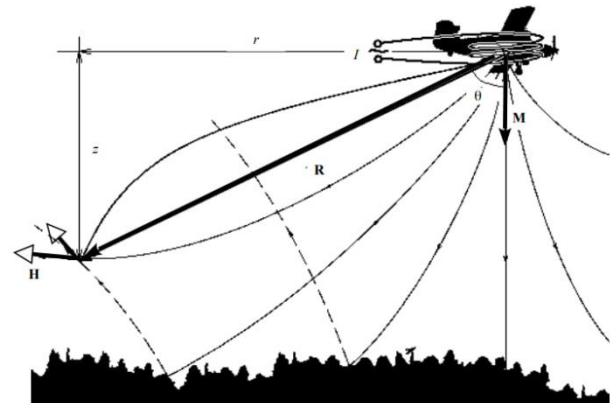


Figure 1. Airborne electromagnetic system EM4H. R - transmitter-receiver radius vector; M - vector of the magnetic moment of the exciting dipole; H - primary field vector.

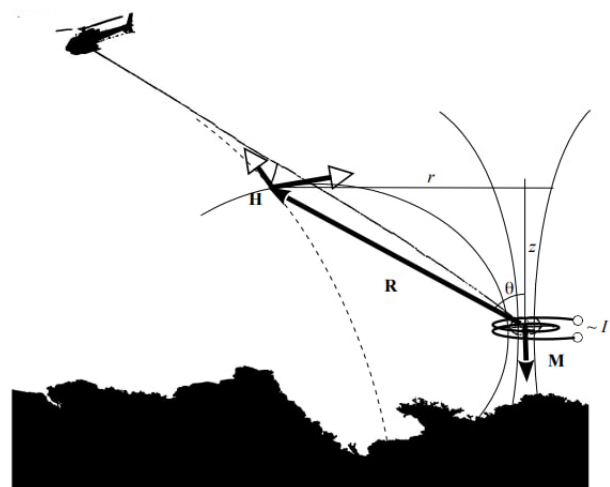


Figure 2. Airborne electromagnetic system EQUATOR.

The EQUATOR (Moilanen et al., 2013) is a system towed behind a helicopter on a cable. The transmitter loop is located in a distance of 70 m from the helicopter, the receiver is attached in the middle of the cable (Figure. 2).

Another choice to make is a type of aircraft to carry the system on. Fixed wing aircraft is more economical, but has to fly at a higher altitude, which results in lower resolution of measurements due to larger footprint of the field source. Helicopter is better suited for survey in the area with complex terrain, but requires more fuel and time for flying over same territory. Some systems take time domain measurements only, others concentrate on frequency domain, and only EQUATOR can do both (Figure 2). There are benefits of each type of measurements (Hodges, 2013), and probably the best approach would be to analyze them in combined regime, as shown in paper (Karshakov et al., 2018).

This paper is devoted to comparison of results of inverting data obtained by three configurations of systems. The first one is frequency domain with four frequencies obtained by fixed wing system EM4H. The second one is towed modification of the same four frequency system, having the same configuration as EQUATOR (Figure 2). The third one is towed system taking measurements in both domains, for which time domain, frequency domain and combined inversion of data has been produced – the EQUATOR.

All three configurations have been tested by the Norilsk branch of A.P. Karpinsky Institute on the same profile, located in the Norilsk region, Russia.

METHOD AND RESULTS

Model formulation

The data used for inversion contain real (in-phase) and imaginary (quadrature) parts of vertical component of secondary magnetic field in frequency domain and averaged in several time gates values of transient decay in time domain. It should be noted that it is difficult to separate primary field and in-phase secondary field, but we can use the differences between the real parts at different frequencies, because both of the systems are calibrated to have the same primary field at all frequencies. Hence the vector of frequency domain measurements has the form

$$\mathbf{Z}_\omega = (\text{Im } \omega_1, \dots, \text{Im } \omega_n, \text{Re } \omega_2 - \text{Re } \omega_3, \dots, \text{Re } \omega_n - \text{Re } \omega_{n-1}), \quad (1)$$

where $\text{Im } \omega_i$ and $\text{Re } \omega_i$ denotes quadrature and in-phase components of response for frequency ω_i .

Corresponding frequencies for EM4H system are 130, 521, 2,083 and 8,333 Hz in both fixed wing and helicopter variant and a range of 25 frequencies from 77

to 15,046 Hz for EQUATOR. Time-domain measurements consist of values of magnetic field derivative dB/dt averaged over fixed time gates. Thus, the measurement vector is

$$\mathbf{Z}_t = (a_1(dB/dt), \dots, a_m(dB/dt)) \quad (2)$$

For EQUATOR system there are 14 time gates a_i ranging from 5 to 4420 μs .

The medium parameters to be estimated from data are those of horizontally layered model (Zhdanov, 2009). The model consisted of 25 layers with fixed thicknesses given by

$$h_i = 4 \cdot 1.1085^{i-1} \text{ m}. \quad (3)$$

Thus, the vector of parameters to be estimated was

$$\mathbf{X} = (\rho_1, \dots, \rho_{25}). \quad (4)$$

The approach to solving the inverse problem, that is, estimating parameters from measurements, taken in this paper, was the Iterated Extended Kalman filter (Karshakov, 2020). This fast and efficient algorithm provides parameter estimates starting from specified initial conditions. In this work a homogeneous half-space has been used for this purpose, with resistivity estimated with the same algorithm based on data for lowest frequencies.

Below are shown inversion results for data obtained from Norilsk region (Figure 3).

Figure 4 shows results of combined inversion of frequency and time domain data for EQUATOR system:

$$\mathbf{Z}_c = (\mathbf{Z}_\omega, \mathbf{Z}_t). \quad (5)$$

The upper graph depicts magnetic field anomaly, given in nT. The next graph shows residuals calculated by formula

$$r = \sqrt{\sum_{i=0}^N \frac{(\tilde{Z}_i - Z_i)^2}{\sigma_i^2}}, \quad (6)$$

where Z_i is i -th component of \mathbf{Z}_c , \tilde{Z}_i is the estimated value of Z_i , σ_i^2 is corresponding noise variance, N is the number of measurements, in the case of combined inversion $N = 2 \cdot n - 1 + m$.

The last part of the figure contains actual inversion data. It can be seen that magnetic anomaly correlates with the resistive body at the depth of 150-200 m.

The descending structures given in the figure correspond to those identified in borehole geological profile several kilometers to the North (Figure 5). It is important to note that the descending conductive layer on the left side of the section in Figure 4 corresponds

well with the P2 coal layer in Figure 5. The sections in Figure 4 and 5 have different horizontal length, but the same vertical exaggeration.

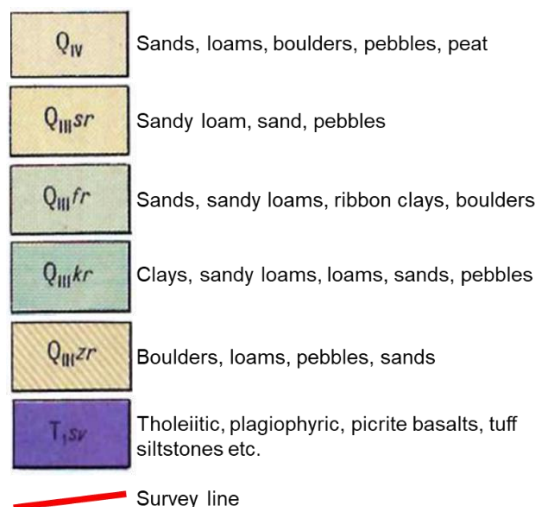


Figure 3. Geological map of the studied region and Survey line (East to West).

Inversion results for other data are compared to figure 4 as a baseline.

Figures 6-9 are organized in the following way. The upper part contains secondary field in time domain (dB_z/dt , Figure 6) or frequency domain ($\text{Im } \omega_i$, Figures 7-9). Figure 10 represents the color legend for the signal arrays. The middle part displays residuals (6) after inversion of the corresponding data. The resistivity sections are presented in the bottom part and have the same colors as the section in Figure 4.

Figure 6 represents time domain inversion results. The structures of the Figure 4 can be clearly seen, but the upper part of the section is much less detailed.

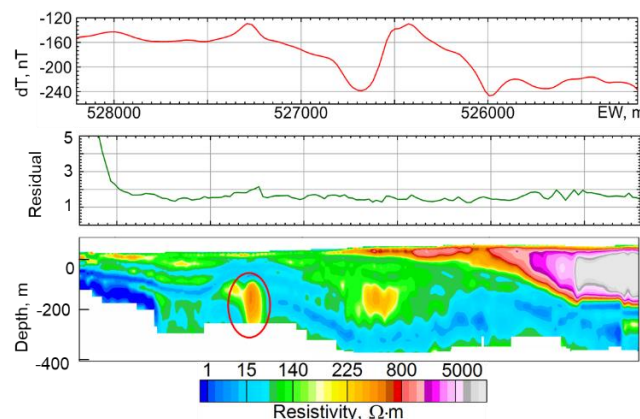


Figure 4. Anomaly magnetic field and results of combined (FD&TD) resistivity inversion.

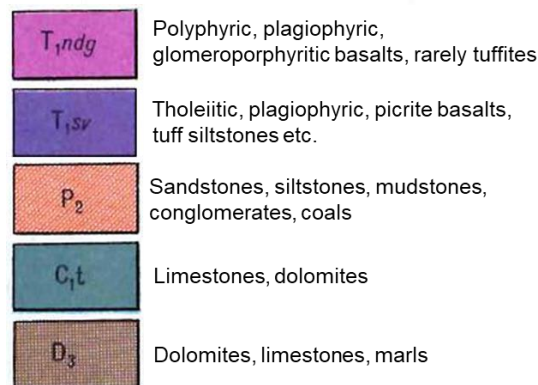
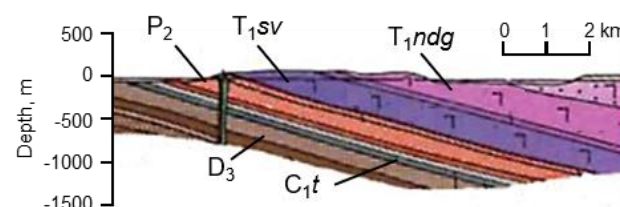


Figure 5. Borehole geological profile in the neighboring area.

Figure 7 provides inversion results for frequency domain data. The resolution of bottom part of profile is lower than that given by time domain, while the detailedness of upper part is higher.

Figure 8 depicts results of inversion for fixed wing configuration of EM4H system, with frequencies in Hz displayed on the right. Note that the resistive body outlined in figure 4 is not seen. The deep parts of profile are almost completely hidden, and the overall resolution is significantly lower. The upper part is less detailed due to lack of frequencies. The investigation depth is lower because of higher base frequency (130 Hz vs. 77 Hz).

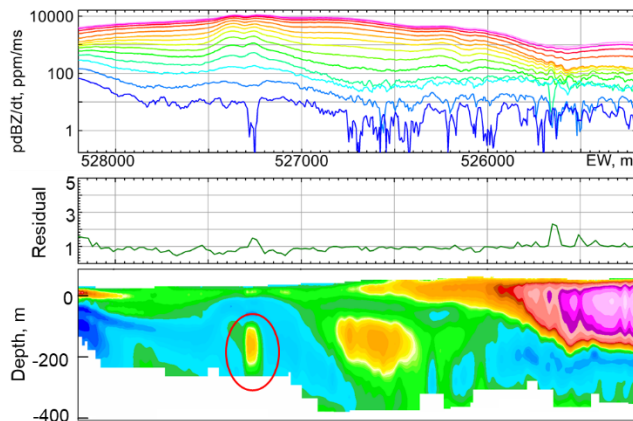


Figure 6. Inversion result for time domain data.

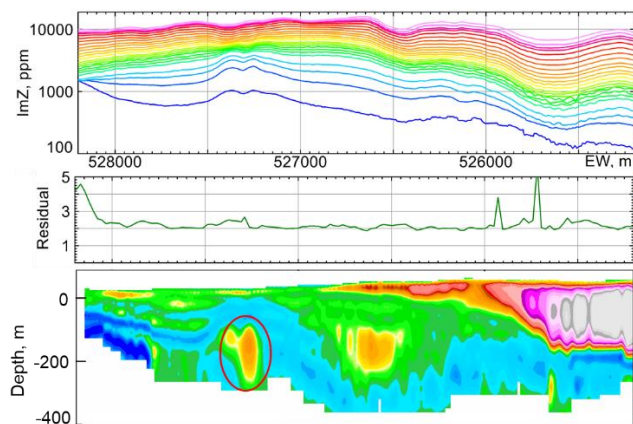


Figure 7. Inversion result for frequency domain data.

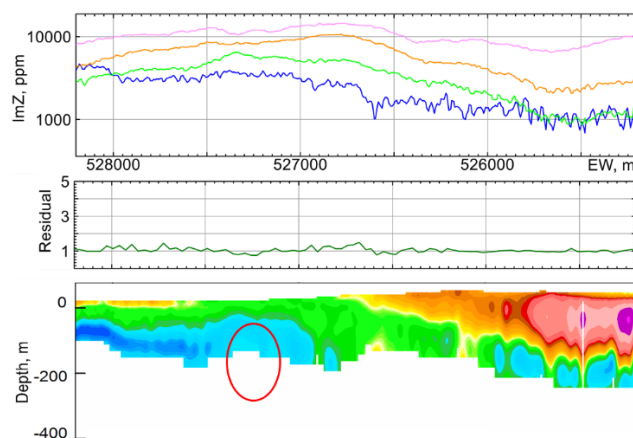


Figure 8. Fixed wing EM4H inversion results.

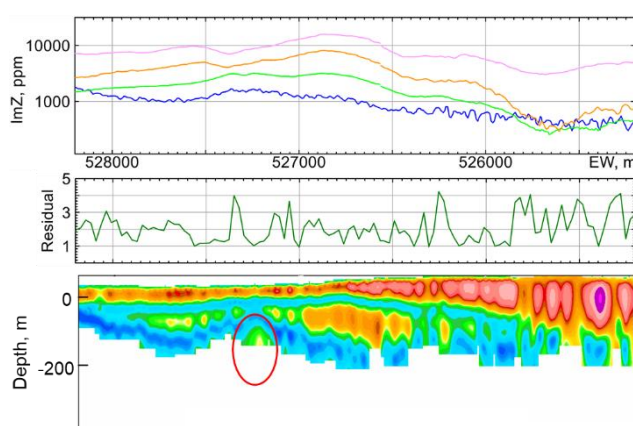


Figure 9. Helicopter EM4H inversion results.

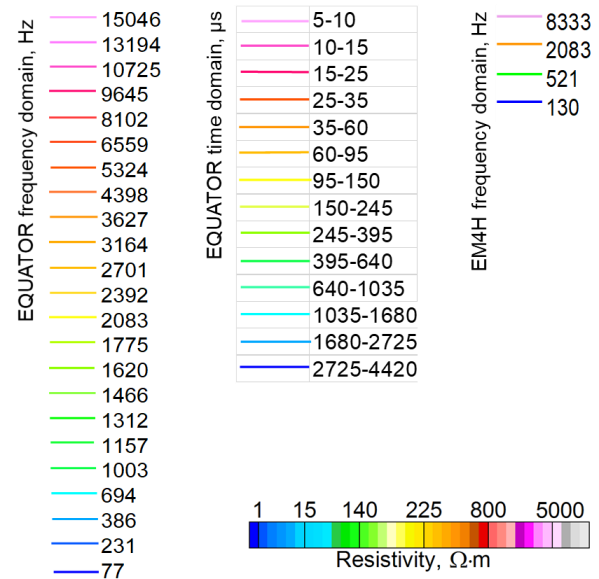


Figure 10. Signals and resistivity color legend.

Finally, figure 9 gives inversion results obtained for helicopter configuration of EM4H. The spatial resolution is comparable to that of EQUATOR, and even the outlined resistive body is seen. But the investigation depth is lower obviously due to higher base frequency (130 Hz vs. 77 Hz).

Also, some sharp resistive contrasts between the upper layers can be seen – a thin conductive layer over a very resistive one. The probable explanation is induced polarization effect, which can be attributed to ice melting. An experienced geophysicist can see it in the right part of the time domain responses (Figure 6). It leads to appearance of higher resistivities in the corresponding part of the section.

The helicopter borne EM4H system was flown in October, while all the other systems flew in the beginning of summer. This may have led to different melting degree.

CONCLUSIONS

In this work we presented results of inverting electromagnetic data for several configurations of AEM system. It has been demonstrated that:

- The highest spatial resolution and the largest exploration depth must be attributed to inversion in combined regime (both time domain and frequency domain data).
- Pure time domain inversion provided detailedness of deeper part of profile, while frequency domain one turned out to be better suited for near-surface exploration.
- The fixed wing EM4H system results correspond well to geological structure of profile, while lacking details.

- Helicopter EM4H system possessed spatial resolution compared to that of EQUATOR, but lead to sharp contrasts between resistivities of neighboring layers. This may be attributed to the fact that the territory is located in permafrost region, and seasonal difference in data collection resulted in occurrence of ice melting, corrupting measurements.
- The data indicated slight presence of induced polarization, which is more visible in EQUATOR data due to detailed frequency spectrum.

REFERENCES

- Hodges, G., 2013, The power of frequency domain: When you should be using it: Extended Abstracts of the 6th International AEM Conference & Exhibition, 5 pp.
- Karshakov, E., Moilanen, E., 2018. Combined interpretation of time domain and frequency domain data. Proceedings of 7th International Workshop on Airborne Electromagnetics, 2018.
- Legault, J.M., 2015. Airborne Electromagnetic Systems - State of the Art and Future Directions. *CSEG Recorder* 40, no. 6: 38-49
- Moilanen, J., Karshakov, E., Volkovitsky, A., 2013. Time Domain Helicopter EM System Equator: Resolution, Sensitivity, Universality. Proceedings of 13th SAGA Biennial Conference and Exhibition, 2013.
- Moilanen, J., 2022. Modern methods of airborne electromagnetic survey. *Izvestiya, Physics of the Solid Earth*, 58(5), 755-764.
- Telford, W., Geldart, L., Sheriff, R., 1990. Applied geophysics. Cambridge university press.
- Volkovitskiy, A., Karshakov, E., Trusov, A., 2008. Four frequency aem system EM-4H. Abstract from 5th International conference on airborne electromagnetics.
- Whitford, M., Fitzpatrick, A., 2023. Some comparisons of AEM systems for specific mineral exploration problems. Proceedings of 8'th International Airborne Electromagnetics Workshop. 231-236.
- Zhdanov, M. S., 2009. Geophysical electromagnetic theory and methods. Elsevier.